

## Porous Manganese Oxide Octahedral Molecular Sieves and Octahedral Layered Materials

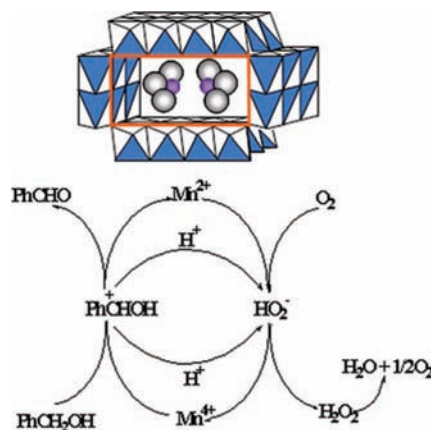
STEVEN L. SUIB\*

Unit 3060, Department of Chemistry, The University of Connecticut,  
55 North Eagleville Road, Storrs, Connecticut 06269-3060

RECEIVED ON JULY 16, 2007

### CON SPECTUS

This Account first gives a historical overview of the development of octahedral molecular sieve (OMS) and octahedral layer (OL) materials based on porous mixed-valent manganese oxides. Unique properties of such systems include excellent semiconductivity and porosity. Materials that are conducting and porous are rare and can offer novel properties not normally available with most molecular sieve materials. The good semiconductivity of OMS and OL systems not only permits potential applications of the conductivity of these materials but also allows characterization of these systems where charging effects are often a problem. Porous manganese oxide natural materials are found as manganese nodules, and these materials when dredged from the ocean floors have been used as excellent adsorbents of metals such as from electroplating wastes and have been shown to be excellent catalysts. Rational for synthesis of novel OMS and OL materials is related to the superb conductivity, microporosity, and catalytic activity of these natural materials. The natural systems are often found as mixtures, are poorly crystalline, and have incredibly diverse compositions due to exposure to various aqueous environments in nature. Such exposure allows ion exchange to occur. Preparation of pure crystalline OL and OMS systems is one of the very significant goals of this work.



The status of this research area is one of moderate development. Opportunities exist for preparation of a multitude of novel materials. Some applications of these materials have recently been achieved primarily in the area of catalysis and membranes, and others such as sensors and adsorptive systems are likely. Characterization studies are becoming more sophisticated as new materials and proper preparation of materials for such characterization studies are being done.

The research area involved in this work is solid state chemistry. The fields of materials synthesis, characterization, and applications of materials are all important in developments of this field. Researchers in chemistry, chemical engineering, materials science, physics, and biological sciences are actively pursuing research in this area.

The most significant results found in this work are related to the novel structural and physical properties of porous manganese oxide materials. Variable pore size materials have been synthesized using structure directors and with a variety of synthetic methodologies. Transformations of tunnel materials with temperature and in specific atmosphere have recently been studied with *in situ* synchrotron methods. Conductivities of these materials appear to be related to the structural properties of these systems with more open structures being less conductive. Catalytic properties of these OMS and OL materials have been shown to be related to the redox cycling of various oxidation states of manganese such as Mn<sup>2+</sup>, Mn<sup>3+</sup>, and Mn<sup>4+</sup>.

Chemists interested in synthesis of new materials, the chemistry of solids, enhancing the rates of catalytic reactions, and finding new applications of materials would be interested in these novel materials. Fundamental properties of electron transfer are critical to this research. Concepts of nonstoichiometry, defects, oxygen vacancies, and intermediates are fundamental to many of the syntheses, characterization, and applications such as fuel cells, catalysis, adsorption, sensors, batteries, and related applications.

## Introduction: Tunnels, Layers, and Controlled Shapes

Dr. David Storm of Texaco Research Laboratories in Beacon, NY, visited our laboratory in 1991, discussed structures of natural manganese oxide nodules,<sup>1</sup> and said that our group should be able to make such materials. Dr. Yanfei Shen spent 2 years trying a variety of syntheses and made a thermally stable  $3 \times 3$  tunnel structure material, which we labeled OMS-1.<sup>2</sup> Interest in OMS-1 stemmed from the 6.9 Å square tunnels, the mixed-valent semiconducting nature, outstanding adsorptive properties, and excellent activity in numerous catalytic reactions. Our major collaborator in this early work was Dr. Chi-Lin O'Young at Texaco Research Laboratories. The long sought after hydrothermal stability of OMS-1 and similar materials was not realized and prevented use of such materials in catalytic cracking. Various structures of octahedral layer (OL) and octahedral molecular sieve (OMS) materials are shown throughout this Account.

Time and many experiments by Professor Zheng Rong Tian would show that the good thermal stability of OMS-1 of about 600 °C was due to incorporation of some  $Mg^{2+}$  into the framework of these tunnel materials.<sup>3</sup> Dr. Tian later designed some crystalline walled manganese oxide mesoporous systems (MOMS) that have interesting adsorptive and catalytic properties.<sup>4</sup>

A key phase that shows outstanding electrochemical and catalytic properties is the  $2 \times 2$  synthetic cryptomelane or OMS-2 structure. Professor Roberto DeGuzman used a combination of ac impedance, dc conductivity, and electrochemical methods to show that electrons could readily flow through OMS materials, in particular OMS-2.<sup>5</sup> Doping of these materials created differences of orders of magnitude in conductivity, and when two electron jumps from doped  $M^{2+}$  to  $Mn^{4+}$  occurred, the conductivity suffered tremendously due to these traps.

A unique structural feature of OMS-2 materials is the myriad of morphologies that can occur. Professor Oscar Giraldo showed that perfect helices of OMS-2 could be formed from nanosize layered precursors after ion exchange and heat treatment while retaining the helical morphology.<sup>6</sup> Elegant high-resolution microscopy experiments by Dr. Michael Tsapatsis of the University of Minnesota and his group showed that these systems are well ordered and crystalline and made up of individual threads like that in a rope.

Such threads when deposited on a flat surface were found by Dr. Jikang Yuan to self-assemble and align.<sup>7</sup> These individual fibers formed inorganic oxide paper or membrane

materials, dubbed protean papers by Dr. Philip Ball of *Nature*,<sup>8</sup> because they are extremely versatile, can be redispersed, and can be cut, written on, and folded. Dr. Yuan also made hollow spheres of OMS-2 that showed excellent enhancement in catalytic oxidation reactions due to enhanced surface area, showing that morphology can lead to changes in catalytic activity.<sup>9</sup>

Dr. Xiongfei Shen, brother of Dr. Yanfei Shen, about 10 years later, showed that a variety of OMS materials having different pore sizes and tunnel structures could be prepared from the same hard cation,  $Na^+$ .<sup>10</sup> These experiments clearly showed that as with zeolites, in many cases structure directors rather than exact templates are used to form OMS materials. Until this time, specific cations were often used to prepare specific tunnel structures, such as  $Rb^+$  for preparation of the  $2 \times 4$  tunnel structure.

Dr. Young Chan Son discovered that OMS-2 materials when treated with acid could markedly catalyze the selective oxidation of alcohols to aldehydes.<sup>11</sup> No overoxidation occurred, and in almost all cases, 100% selectivity was obtained. This is in marked contrast to stoichiometric oxidations using active manganese oxide. A redox Mars van Krevelen mechanism was proposed based on kinetic, O-labeling, and D/H-labeling experiments.<sup>12a</sup>

Dr. Oscar Giraldo showed that the rate of transport for ion exchange in thin films of OMS-2 was markedly enhanced.<sup>12b</sup> Interconnection of mesopores and micropores in these materials was invoked to explain the ultrafast rate ( $<1$  s) for 100% exchange. This enhanced mass transport may be partially responsible for the high rates of reaction of these materials in selective oxidations.

Drs. Yuan and Li spearheaded recent work to control morphology and growth of OMS materials.<sup>13</sup> In this case, control of the growth rate of OMS-2 was done by adding small amounts of chromium, which slowed the growth rate and made unusual inorganic dendrites. Such highly ordered three-dimensional structures form due to control of the redox potential of small amounts of chromium additives creating a  $Cr_2O_7^{2-}/Cr^{3+}$  couple that is only slightly larger than the  $Mn^{4+}/Mn^{2+}$  couple. This allows precise control over nucleation and growth processes leading to highly uniform dendritic structures.<sup>14</sup>

Recent characterization studies by Xiongfei Shen in collaboration with Jon Hanson of Brookhaven National Laboratory involve *in situ* synchrotron diffraction studies.<sup>15</sup> These time-resolved experiments (Figure 1) show 3-D plots of  $2\theta$ , intensity, and numbers of scans and allow *in situ* determination of changes in structure that provide valuable information regard-

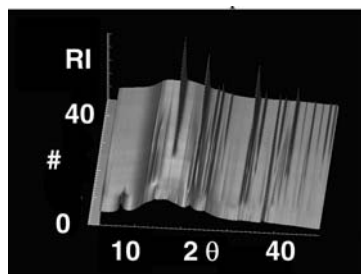


**FIGURE 1.** *In situ* synchrotron diffraction of formation of  $1 \times 2$  tunnel structure, plot of relative intensity (RI), number of scans, and angle of diffraction,  $2\theta$ . Reproduced from ref 15. Copyright 2006 American Chemical Society.

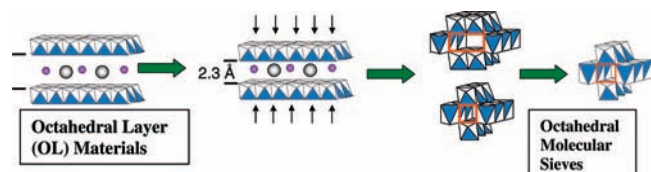


**FIGURE 2.** Results of *in situ* synchrotron diffraction, layer to tunnel transformation studies. Adapted from ref 15. Copyright 2006 American Chemical Society.

ing phase changes, thermal stabilities, intermediates, and mechanisms of tunnel formation and transformations (Figure 2). Similar *in situ* synchrotron diffraction experiments of the synthesis of OMS-2 show that this phase is formed almost immediately and the numerous changes in the development of structures of the  $1 \times 2$  materials shown in Figure 1 do not occur. Continuing studies involve Rietveld refinements of time-resolved diffraction data of various intermediates.

These *in situ* synchrotron diffraction studies clearly show that as temperature increases there is a closing of pores until only the smallest  $1 \times 1$  tunnel structure is produced. These studies also confirm that there is a transformation from the layered OL-1 structure to tunnel structures. Intensity data taken at various stages suggest that dissolution is minimal and that a solid to solid transformation is likely occurring.

### Perspective: Current Studies

The interaction of nanosize particulates is critical for the controlled deposition of OMS and OL structures. By using mixed aqueous–nonaqueous solvents, Drs. Oscar Giraldo and Jason Durand recently used phase-transfer syntheses to control the size and shape of nanosize particles of OMS and OL materials.<sup>16</sup> One goal of this work was to provide a safe synthesis that would yield small nanosize manganese oxide porous layered and tunnel structure materials and to use these as precursors for syntheses of other materials. This route avoids the use of tetralkylammonium permanganate salts, which can be explosive.<sup>16</sup> Figure 3 shows the formation of layered nanosize particulates from such phase transfer syntheses. As con-

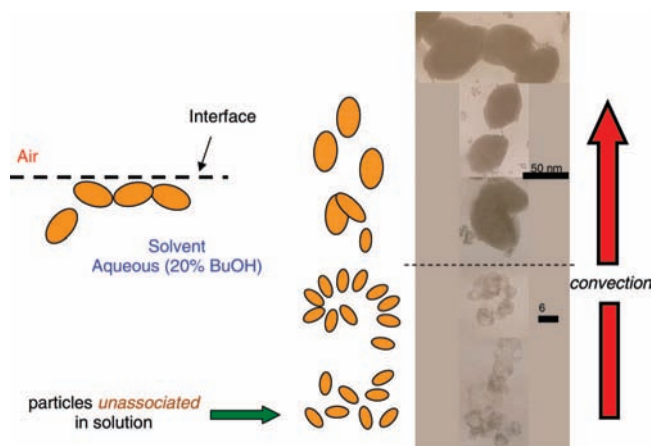


**FIGURE 3.** Particle behavior during formation of nanosize particles of OL-1. Taken from ref 16b.

vection occurs, the originally 6 nm sized OL-1 particles grow to about 50 nm at the air–solvent interface. Shapes of these particles have also been investigated with small angle neutron scattering methods and determined to be two-dimensional ellipsoids. Consistent with calorimetric experiments in collaboration with Dr. Alex Navrotsky, the OL-1 phase is most stable and initially forms in these and many other syntheses.<sup>17</sup>

The novelty of such phase-transfer syntheses is that nanosize precursors as small as 5–10 Å can be prepared that are stable for months. These sizes were determined from a variety of experiments including small angle neutron scattering studies and cryo-transmission electron microscopy studies. Such precursors have been used to make unique materials with unusual morphologies such as inorganic helices,<sup>6</sup> which are quite rare. In addition, nanosize lines of porous manganese oxides<sup>16</sup> and other metal oxides<sup>18</sup> can be prepared from such precursors.

Besides control of size, shape, and structure, there is interest in controlling physical properties of such systems. Conductivity is a unique feature of OL-1 and OMS-1 materials. Both ionic and electrical conductivity can exist in these systems. Recent conductivity experiments by Dr. Josie Villegas have shown a systematic relationship to the structure of tunnel materials. Recent unpublished data clearly show a trend between the types of tunnels in OMS materials and the conductivity. This relationship is shown in Figure 4.

The primary effect on electrical conductivity appears to be the size of the tunnels, although compositional differences, framework substitutions, tunnel compositions, and morphologies cause secondary effects on conductivity. Multielectron transfers induced by divalent substitutions for quadrivalent ions clearly act as traps and severely decrease conductivity. The effects of framework substitutions in a series of structures



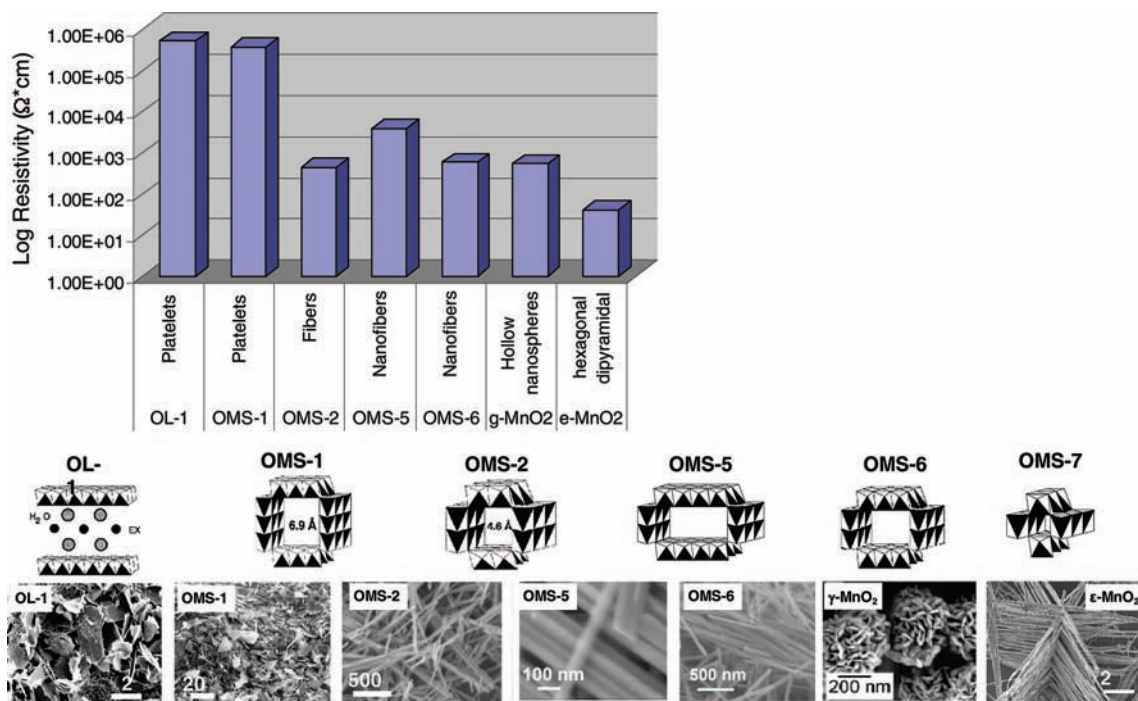


**FIGURE 4.** Resistivity values for various OMS materials. Corresponding structures and morphologies are below, in same order. Taken from ref 19a.

such as those shown in Figure 4, still need to be systematically studied to understand the exact mechanism of conductivity and the roles of defects, electron transfer, and structure. Enhancement of conductivity is crucial to a variety of areas including fuel cell electrodes,<sup>19</sup> battery materials,<sup>20</sup> redox catalysis,<sup>21</sup> electrocatalysis,<sup>22</sup> and sensing devices.<sup>23</sup> The limits of conductivity in these systems need to be determined. Battery work is a current intense subject of interest and involves varying chemical composition of electrodes, generation of higher voltage materials, batteries with enhanced power, systems that recharge at a faster rate, and operation under a wide variety of environmental conditions.

Molecular design of porous materials with novel magnetic properties is also an area of current interest. Fe<sup>3+</sup>-doped framework OMS-2 materials [designated [Fe<sup>3+</sup>]OMS-2] have been prepared that show unique magnetic properties. Framework doping has been done by a sol-gel-assisted combustion method using nitrate precursors and a cross-linking agent. The morphologies of the rods that are formed are novel and thicker than nondoped materials. After doping, the powder is attracted to poles of a magnet (Figure 5). This material also shows semiconducting behavior. Materials that show both semiconducting and ferromagnetic behavior are very uncommon and may be useful for spintronic and other applications.<sup>24,25</sup> Such tunable ferromagnetic semiconductors with Curie temperatures ( $T_c$ 's) above room temperature are unprecedented. This approach of using manganese as a host

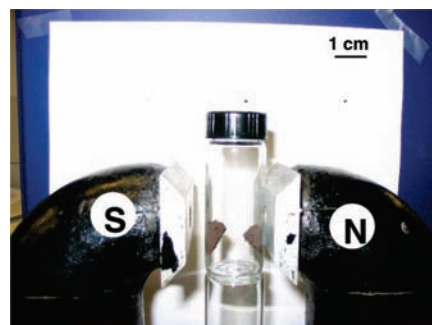


**FIGURE 5.** [Fe<sup>3+</sup>]OMS-2, Mn/Fe = 5, magnetic studies. Taken from ref 10b.

and doping with Fe<sup>3+</sup> is in direct contrast to the low  $T_c$  systems where small amounts of manganese are doped into various semiconductors.<sup>26</sup>

The presence of ferromagnetism in these [Fe<sup>3+</sup>]OMS-2 materials is apparent from magnetic susceptibility experiments (Figure 6). The ferromagnetism can be observed at temperatures as high as 400 °C. This is truly unique behavior. In addition, the dopant level controls the  $T_c$  of these materials, that is, the highest temperature at which ferromagnetism exists above which it then converts to paramagnetic behavior. This control of  $T_c$  with the dopant [Fe<sup>3+</sup>] is unprecedented.

The observed  $T_c$  values do not correspond to any known iron oxide, iron, manganese, or manganese oxide phase, indicating that this behavior is related to the [Fe<sup>3+</sup>] dopant level. Ratios of Fe and Mn and preparation temperatures are given as insets in the upper left side of the panels in Figure 6.

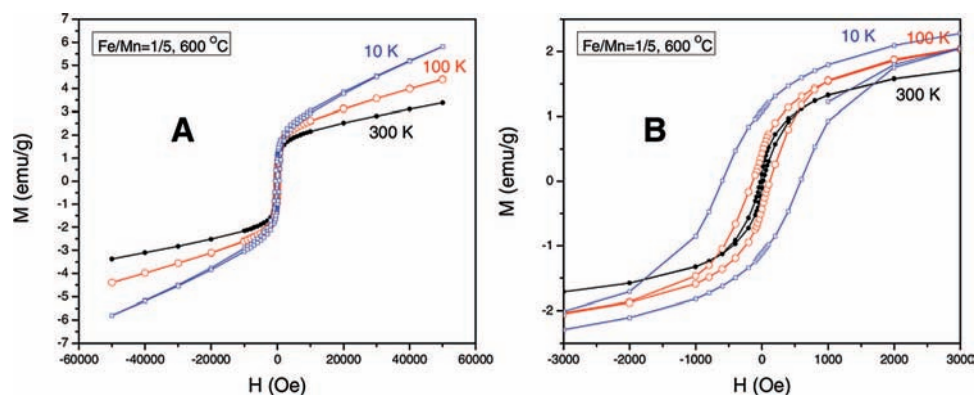


**FIGURE 6.** Magnetic susceptibility of  $[\text{Fe}^{3+}]$ OMS-2 indicative of ferromagnetism: panel B is a magnification of a portion of panel A. Taken from ref 10b.

**TABLE 1.** Dependence of  $T_c$  on  $\text{Fe}^{3+}$  Concentration in  $[\text{Fe}^{3+}]$ OMS-2

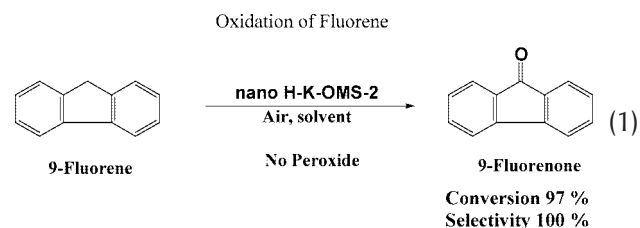
Fe/Mn ratio (atomic)	0	1/10	1/5
Fe wt %	0	5.3%	10%
$T_c$ ( $^{\circ}\text{C}$ )	N/A	360	400

Table 1 shows that the  $T_c$  value changes with the level of iron dopant, which suggests that these signals are not due to impurity phases.  $T_c$  cannot be readily determined for the 1/2 Fe/Mn material since this transition is very broad. Syntheses of  $\text{Fe}^{3+}$  framework doping in other OMS and in OL materials like OL-1, OL-2,  $1 \times 1$ ,  $2 \times 2$  (OMS-2),  $2 \times 3$ ,  $2 \times 4$ ,  $3 \times 3$  (OMS-1) and others are being done to study structural and pore size effects on magnetic properties.

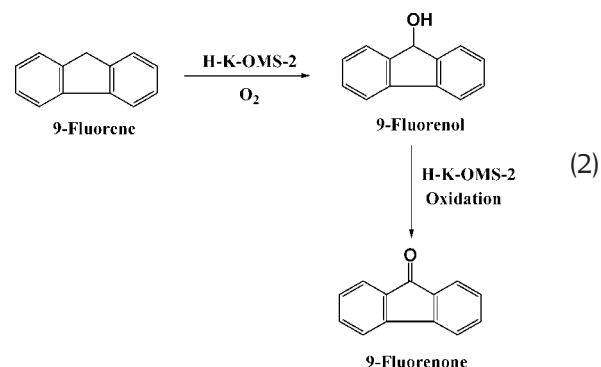
Variable temperature (4  $^{\circ}\text{C}$  to room temperature) Mössbauer studies of the  $\text{Fe}^{3+}$  framework doped materials suggest that the  $\text{Fe}^{3+}$  ions are in high-spin octahedral environments and do not couple at and above room temperature. This is quite interesting and implies that the ferromagnetism results from either Fe–O–Mn or Mn–O–Mn interactions. The latter could be caused by changes in orbital interactions due to strain induced by iron doping. Anomalous synchrotron diffraction, extended x-ray absorption fine structure (EXAFS), and X-ray absorption near edge structure (XANES) experiments are being used to give a better idea of what is exactly going on in these systems. Based on mixed-valent manganese oxides, a new group of spintronics materials has been fabricated by doping  $\text{Fe}^{3+}$  into the KOMS-2 structure. Magnetic, compositional, and microscopy measurements show that the ferromagnetism is not due to impurity phases.

Control of chemical properties is also crucial in many areas such as catalysis. The following section summarizes some recent novel unpublished results in the area of selective oxidations that we are pursuing. The effect of morphology of OMS and OL materials on catalytic selective oxidations is a subject of current interest. With OMS-2 alone there are vari-

ous morphologies such as hollow spheres, helices, papers/membranes, stars, multipods, and dendrites that have the same composition but very different rates of reactions. These rate differences cannot be accounted for solely on the basis of surface areas. Correlations of types and sizes of pores, chemical compositions, and average oxidations states with rates need to be considered for the reactions (eqs 1 and 2) shown below. These reactions are environmentally friendly, generally one-pot, and use air or oxygen as oxidizing agents. Systematic studies of various single and multiple framework-substituted OMS systems with and without  $\text{H}^+$  sites are currently under investigation. The catalysts listed for each reaction are the most active in these reactions to date.



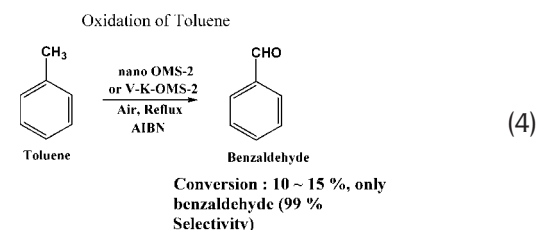
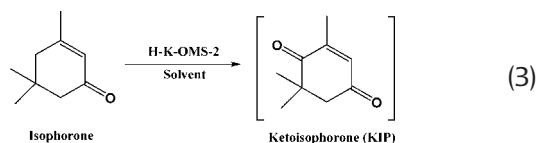
#### Proposed Mechanism of Fluorene Oxidation



A detailed mechanism of the reaction 1 will provide ideas for several oxidation applications. Nano-H-K-OMS-2 particles are critical to this reactivity. Almost no conversion occurs with larger particles ( $> 500 \text{ \AA}$ ) of H-K-OMS-2. A proposed mecha-

nism is given in eq 2, although the 9-fluorenol intermediate cannot yet be isolated. Fluorenone has been identified as a model compound capable of modifying a wide variety of polymeric substrates.<sup>27a</sup> For example, fluorenone chromophore has been incorporated into the backbone of Nylon.<sup>27</sup> Mass spectrometry, FTIR, and NMR methods are being used to study this mechanism. Production of oxygenates at a saturated position without peroxide is extremely difficult, and this is an impetus for studying this reaction mechanism. The first step is not well-established, but hydrogen is most likely coming from H-K-OMS-2. As can be seen above, the most active catalysts are obtained when Brønsted acidity is introduced into these  $2 \times 2$  materials.

Activation of hydrocarbons is the first step in petrochemical reactions like polymerization. Activation of toluene is not readily catalyzed in selective oxidations. Peroxide has not been used in reaction 4. Toluene is used as the solvent and reactant.



Reaction 4 has been demonstrated to occur over nano-size OMS-2 and V-K-OMS-2 catalysts with 10% selectivity. Usually high temperature, high pressure, and strong acids are used to drive this reaction, and low selectivities are typically observed with non-OMS systems. The conditions for reaction 4 are quite mild without strong acid or unnecessary solvents.

The reactions are catalyzed by a variety of materials. In many cases (reactions 2 and 3), Brønsted acidity appears to be very important. In other cases like reaction 4, incorporation of metals like V into framework sites enhances the rate of these reactions. In addition, particle size effects, in particular nanosize catalysts, often increase the rates of these reactions.

There is considerable debate about the active sites in these selective oxidations concerning OMS and OL catalysts. Other catalysts known to drive these reactions are believed to proceed by base-catalyzed mechanisms, and in the gas phase, radicals are invoked. The OMS and OL catalysts have higher

rates when Brønsted acid sites are introduced.<sup>11,12</sup> Brønsted acid sites are due to incorporation or generation of  $\text{H}^+$ . Another key feature is that radical scavengers, rather than slowing down such reactions, are actually oxidized by these catalysts. Redox cycling of the mixed-valent manganese oxidation states is suggested since when oxygen is removed from the feed, oxidation of the catalyst occurs and activity stops. Average oxidation state potentiometric titration data also clearly show changes in oxidation states in these materials, unless oxygen is present. The loss of lattice oxygen during reaction is believed to be an important process in these reactions and is shown by  $^{18}\text{O}_2$  labeling experiments and concomitant *in situ* XRD experiments. Finally, the selectivity in such reactions is unprecedented.

## Synthesis Strategies

There are several strategies for making various phases discussed throughout this manuscript. There is no *a priori* strategy for making any particular material. One key technique is to build up materials from the smallest possible units. The phase transfer synthesis described above for making small nanosize colloidal particles is useful in this context; however, the thermodynamically favored layered structure (OL-1) is almost always formed first. Conversion of the layered phase into tunnel structures is often a path that must be taken. Isomorphous substitution such as the case of the magnetic materials resulting from iron being incorporated in framework sites needs to be synthesized *in situ* before nucleation. As in most syntheses, size, charge, and polarizability of various cations and anions must be considered as well as many other factors like solubility, role of solvent, physical conditions of temperature and others, stable coordination numbers, solvation effects, and others. There are very few cases of true template effects. Most materials are structure-directed by a variety of inorganic and organic structure directors. An exception seems to be the role of  $\text{Mg}^{2+}$  in the preparation of thermally stable OMS-1 materials.

In the case of the  $2 \times 2$  OMS-2 tunnel structure material, a variety of methods have been used for synthesis of this system, such as sol-gel, high-temperature, hydrothermal, microwave, phase-transfer, solvent-free, reflux, and other methods. Catalytic studies suggest that each of these different chemical preparation methods can lead to materials that are not exactly the same. There are many possible novel synthetic methods that could be tried to make a variety of novel OL and OMS type materials. Epitaxial growth is one method that comes to mind that has not yet been exploited.



## Conclusions

Control of the conductivity and electron-transfer capability of solids is crucial to a number of areas like fuel cell electrodes,<sup>28</sup> batteries,<sup>29</sup> redox catalysis,<sup>30</sup> and artificial biological systems.<sup>31</sup> Knowledge of redox properties is key to understanding how enzymes achieve efficient transport of electrons across biological membranes.<sup>32</sup> Membranes with embedded proteins are used by nature to move electrons to critical sites to support life processes.<sup>33</sup> Mimicking such membrane composites provides a powerful approach to explore redox chemistry in biomimetic microenvironments.<sup>34</sup> Mixed valence is important in such biological systems, as well as the OMS, OL, and other systems described. The nomenclature used throughout this paper of OMS-1, OMS-2, etc. refers to the order in which such materials were discovered and here refer to the  $3 \times 3$  and  $2 \times 2$  materials, respectively. Some recent examples from the literature of other groups who are applying OMS systems include zinc air batteries,<sup>35</sup> low-temperature adsorption of  $\text{SO}_2$ , CO, and NO oxidation,<sup>36</sup> and amperometric biosensors of glucose oxidase.<sup>37</sup> New syntheses of OMS, OL, and related materials will likely exploit the redox properties of various reagents. Control of particle size, morphology, composition, oxidation states, and concomitant properties should be realized.

Fundamental knowledge in the areas of synthesis, new characterization methods, structural analysis, mixed valency, electron transfer, magnetic behavior, conductivity, catalysis, electrocatalysis, and photocatalysis has been obtained in our studies of OMS and OL materials. The novelty of porous semiconducting molecular sieves has allowed fundamental studies of effects of electron transfer<sup>11,12</sup> and unique electrocatalytic systems<sup>38</sup> based on nanofilms of OL and OMS. Control and understanding of conductivity<sup>4-6</sup> of all of these materials is important for redox catalytic cycling, sensing devices, and several spectroscopic and microscopic experiments where charging can be significantly reduced. Synchrotron, high-resolution spectroscopic, microscopic, and imaging studies have led to an excellent understanding of many of the fundamental structural transformations and electronic features of these systems.<sup>7,9,10,15,16</sup> Catalytic studies have led to correlations of structure/activity/selectivity, shape selectivity, and redox or electron transfer capability.<sup>11,12</sup> How electrons are moved in such systems is critical as regards possible applications of these materials.

Unique features of the systems described above include the myriad of morphologies available in these systems (helices, nanoropes, stars, dendrites, nanowires, nanolines, nanopat-

terns, nanospheres), a variety of tunnel structures ( $1 \times 1$ ,  $1 \times 2$ ,  $2 \times 2$ ,  $3 \times 3$ ,  $2 \times 4$ ,  $3 \times 5$ ), excellent conductivity, ease of ion exchange, and protean free-standing papers as catalytic and adsorptive materials.<sup>7,8</sup> Lithium intercalation has led to unique battery and sensor systems that are functional and low cost. Lithium air batteries are primary batteries. Recent attempts have been made to prepare  $\lambda$ - $\text{MnO}_2$  phases that are reversible so that these systems can be used in rechargeable secondary batteries.<sup>39</sup> Many of the OL and OMS materials discussed in this proposal are being tested at Yardney, Inc. as both primary and secondary battery systems. Control of morphologies and exploitation of these properties in real devices will likely be the focus of future work.

Catalytic oxidations are the focus of proposed catalysis studies because excellent preliminary results and selected high impact targets have been obtained.<sup>1-12</sup> There is continued interest in both producing and scaling OMS and OL materials. Recent work from others concerning generation of  $3 \times 3$  materials using bacterial catalysis,<sup>40</sup> production of single-crystal multipods of  $\text{MnO}$ ,<sup>41</sup> generation of macroporous manganese oxides with regenerative mesopores,<sup>42</sup> and production of redox active nanosheet crystallites of  $\text{MnO}_2$  via delamination<sup>43</sup> and others already cited have provided considerable insight and research thrusts for the future. The unique combination of availability of numerous structural types, good electrical properties, high permeability, and high porosity is rare. OMS, OL, and related materials offer these novel properties that are not readily available in other systems (zeolites, pillared clays, clays). Extensions to non-manganese-based porous nanomaterials are also underway. The selectivities and stabilities of many of the catalysts described here are unprecedented. Applications in thermal, photo-, and electrocatalysis have been summarized. Future studies may lead to improved conversions and rates of reaction as well as novel applications.

*We acknowledge the U.S. Department of Energy, Office of Basic Energy Sciences, for support of most of our research.*

---

## BIOGRAPHICAL INFORMATION

**Steven L. Suib** was born in western New York State where he obtained a B.S. degree in chemistry and geology at the State University College of New York at Fredonia. His graduate work was done at the University of Illinois at Urbana-Champaign with Galen D. Stucky. His postdoctoral work was done at Illinois with Larry R. Faulkner. He joined the faculty of the Department of Chemistry at the University of Connecticut in 1980 where he is currently Board of Trustees Distinguished Professor.

FOOTNOTES

\*Phone (860)-486-2797; fax (860)-486-2981; e-mail Steven.Suib@Uconn.edu.

REFERENCES

1 (a) Turner, S.; Buseck, P. R. Todorokites: a new family of naturally occurring manganese oxides. *Science* **1981**, *212* (4498), 1024–1027. (b) Turner, S.; Siegel, M. D.; Buseck, P. R. Structural features of todorokite intergrowths in manganese nodules. *Nature* **1982**, *296* (5860), 841–842.

2 Shen, Y. F.; Zenger, R. P.; DeGuzman, R.; Suib, S. L.; McCurdy, L.; Potter, D. I.; O'Young, C. L. Octahedral molecular sieves: Synthesis, characterization and applications. *Science* **1993**, *260*, 511–515.

3 Tian, Z. R.; Yin, Y. G.; Suib, S. L.; O'Young, C. L. Effects of Mg<sup>2+</sup> ions on the formation of todorokite type manganese oxide octahedral molecular sieves. *Chem. Mater.* **1997**, *9*, 126–1133.

4 Tian, Z. R.; Tong, W.; Wang, J. Y.; Duan, N.; Krishnan, V. V.; Suib, S. L. Manganese oxide mesoporous structures: Mixed valent semiconducting catalysts. *Science* **1997**, *276*, 926–930.

5 DeGuzman, R. N.; Awaluddin, A.; Shen, Y. F.; Tian, Z. R.; Suib, S. L.; Ching, S.; O'Young, C. L. Electrical resistivity measurements on manganese oxides with layer and tunnel structures: Birnessites, todorokites, and cryptomelanes. *Chem. Mater.* **1995**, *7*, 1286–1292.

6 Giraldo, O.; Brock, S. L.; Marquez, M.; Suib, S. L.; Hillhouse, H.; Tsapatsis, M. Spontaneous formation of inorganic helices. *Nature* **2000**, *405*, 38.

7 Yuan, J.; Gomez, S.; Villegas, J.; Laubernds, K.; Suib, S. L. Spontaneous formation of inorganic paper-like materials. *Adv. Mater.* **2004**, *16*, 1729–1732.

8 Ball, P. Protean paper. *Nature* **2004**, *432*, 288.

9 Yuan, J.; Laubernds, K.; Zhang, Q.; Suib, S. L. Self-assembly of microporous manganese oxide octahedral molecular sieve hexagonal flakes into mesoporous hollow nanospheres. *J. Am. Chem. Soc.* **2003**, *125*, 4966–4967.

10 (a) Shen, X.; Ding, Y.; Liu, J.; Cai, J.; Laubernds, K.; Zenger, R. P.; Vasiliev, A.; Aindow, M.; Suib, S. L. Control of Nano-scale Tunnel Sizes of Porous Manganese Oxide Octahedral Molecular Sieve (OMS) Nanomaterials. *Adv. Mater.* **2005**, *17*, 805–809. (b) Shen, X. Ph.D. Thesis, University of Connecticut, Storrs, CT, 2006.

11 Son, Y. C.; Makwana, V. D.; Howell, A. R.; Suib, S. L. Efficient, catalytic, aerobic oxidation of alcohols with octahedral molecular sieves. *Angew. Chem., Int. Ed.* **2001**, *40*, 4280–4283.

12 (a) Makwana, V. D.; Son, Y. C.; Howell, A. R.; Suib, S. L. The role of lattice oxygen in selective benzyl alcohol oxidation using OMS-2 catalyst: A kinetic and isotope-labeling study. *J. Catal.* **2002**, *210*, 46–52. (b) Giraldo, O.; Brock, S. L.; Willis, W. S.; Marquez, M.; Suib, S. L. Manganese oxide thin films with fast ion-exchange properties. *J. Am. Chem. Soc.* **2000**, *122*, 9330–9331.

13 Yuan, J.; Li, W.; Gomez, S.; Suib, S. L. Shape-controlled synthesis of manganese oxide octahedral molecular sieve three-dimensional nanostructures. *J. Am. Chem. Soc.* **2005**, *127*, 14184–14185.

14 Hurlley, S. Chemistry: Inorganic dendrites. *Science* **2005**, *310*, 197.

15 Shen, X.; Hanson, J.; Suib, S. L. *In-situ* synthesis of mixed-valent manganese oxide nanocrystals: An *in-situ* synchrotron X-ray diffraction study. *J. Am. Chem. Soc.* **2006**, *128*, 4570–4571.

16 (a) Giraldo, O.; Durand, J. P.; Ramanan, H.; Laubernds, K.; Suib, S. L.; Tsapatsis, M.; Brock, S. L.; Marquez, M. Dynamic organization of inorganic nanoparticles into periodic micrometer-scale patterns. *Angew. Chem., Int. Ed.* **2003**, *42*, 2905–2909. (b) Durand, J. Ph.D. Thesis, University of Connecticut, Storrs, CT, 2007.

17 Cai, J.; Suib, S. L.; Navrotsky, A. Framework doping of iron in tunnel structure cryptomelane. *Chem. Mater.* **2001**, *13*, 2413–2422.

18 Calvert, C.; Burke, K. A.; Suib, S. L. Spontaneous and self-assembled line formations on silicon substrates using vanadium pentoxide sol–gels. *J. Phys. Chem. B* **2005**, *109*, 22685–22691.

19 (a) Villegas, J. Ph.D. Thesis, University of Connecticut, Storrs, CT, 2006. (b) Ruiz-Morales, J. C.; Canales-Vazquez, J.; Savaniu, C.; Marrero-Lopez, D.; Zhou, W.; Irvine, J. T. S. Disruption of extended defects in solid oxide fuel cell anodes for methane oxidation. *Nature* **2006**, *439*, 568–571. (c) Song, Y.; Xu, H.; Wei, Y.; Kunz, H. R.; Bonville, L. J.; Fenton, J. M. Dependence of high-temperature PEM fuel cell performance on Nafion content. *J. Power Sources* **2006**, *154*, 138–144. (d) Chu, Y. H.; Ahn, S. W.; Kim, D. Y.; Kim, H. J.; Shul, Y. G.; Han, H. Combinatorial investigation of Pt-Ru-M as anode electrocatalyst for direct methanol fuel cell. *Catal. Today* **2006**, *111*, 176–181.

20 Ogasawara, T.; Debart, A.; Holzapfel, M.; Novak, P.; Bruce, P. G. Rechargeable Li<sub>2</sub>O<sub>2</sub> electrode for lithium batteries. *J. Am. Chem. Soc.* **2006**, *128*, 1390–1393.

21 (a) Heracleous, E.; Lemonidou, A. A. Ni-Nb-O mixed oxides as highly active and selective catalysts for ethene production via ethane oxidative dehydrogenation. Part II: Mechanistic aspects and kinetic modeling. *J. Catal.* **2006**, *237*, 175–189. (b)

Herrmann, J. M. The electronic factor and related redox processes in oxidation catalysis. *Catal. Today* **2006**, *112*, 73–77.

22 (a) Machida, M.; Sato, K.; Ishibashi, I.; Abul, H. M.; Ikeue, K. Electrocatalytic nitrate hydrogenation over a H<sup>+</sup>-conducting solid polymer electrolyte membrane-modified cathode assembly. *Chem. Commun.* **2006**, *7*, 732–734. (b) Neophytides, S. G.; Murase, K.; Zafeirotas, S.; Papakonstantinou, G.; Paloukis, F. E.; Krstajic, N. V.; Jaksic, M. M. Composite hypo-hyper-d-intermetallic and interionic phases as supported interactive electrocatalysts. *J. Phys. Chem. B* **2006**, *110*, 3030–3042.

23 (a) Acevedo, D. F.; Balach, J.; Rivarola, C. R.; Miras, M. C.; Barbero Ce., A. Functionalised conjugated materials as building blocks of electronic nanostructures. *Faraday Discuss.* **2006**, *131*, 235–252. (b) Shimizu, Y. Design of novel electrochemical sensor device with ceramic functional electrode. *Chem. Sens.* **2005**, *21*, 24–32.

24 (a) Zutic, I.; Fuhrer, M. Spintronics: A path to spin logic. *Nature Phys.* **2005**, *1*, 85–86. (b) Gallagher, W. J.; Parkin, S. S. P. *IBM J. Res. Rev.* **2006**, *50*. (c) Cowburn, R.; Petit, D. Spintronics: turbulence ahead. *Nat. Mater.* **2005**, *4*, 721–722.

25 (a) Beach, G. S. D.; Nistor, C.; Knutson, C.; Tsoi, M.; Erskine, J. L. Dynamics of field-driven domain-wall propagation in ferromagnetic nanowires. *Nat. Mater.* **2005**, *4*, 741–744. (b) Bellani, V.; Stella, A.; Chen, C.; Wang, X. Optical properties of Cd<sub>1-x</sub>MnxTe/Cd<sub>1-y</sub>MnyTe superlattices with high difference of Mn concentration between wells and barriers. *J. Appl. Phys.* **2005**, *97*, 083526.

26 (a) Dietl, T. Functional Ferromagnets. *Nat. Mater.* **2003**, *2*, 646–648. (b) Liu, C.; Yun, F.; Xia, B.; Cho, S. J.; Moon, Y. T. Structural analysis of ferromagnetic Mn-doped ZnO thin films deposited by radio frequency magnetron sputtering. *J. Appl. Phys.* **2005**, *97*, 126107.

27 (a) Blencowe, A.; Cosstick, K.; Hayes, W. Surface modification of nylon 6,6 using a carbene insertion approach. *New J. Chem.* **2006**, *30*, 53–58. (b) Walte, M. E.; Kolonko, R. P.; Wehmyer, R. M. US Patent 5,545,760, 1997.

28 Boukamp, B. A. Fuel cells: The amazing perovskite anode. *Nat. Mater.* **2003**, *2*, 294–296.

29 (a) Zhou, W. C.; Yang, H. X.; Shao, S. Y.; Ai, X. P.; Cao, Y. L. Superior high rate capability of tin phosphide used as high capacity anode for aqueous primary batteries. *Electrochem. Commun.* **2006**, *8*, 55–59. (b) Dominko, R.; Bele, M.; Gaberscek, M.; Meden, A.; Remskar, M.; Jamnik, J. Structure and electrochemical performance of Li<sub>2</sub>MnSiO<sub>4</sub> and Li<sub>2</sub>FeSiO<sub>4</sub> as potential Li- battery cathode materials. *Electrochem. Commun.* **2006**, *8*, 217–222.

30 (a) Costentin, C.; Robert, M.; Saveant, J. M. Does catalysis of reductive dechlorination of tetra- and trichloroethylenes by vitamin B12 and corrinoid-based dehalogenases follow an electron transfer mechanism. *J. Am. Chem. Soc.* **2005**, *127*, 12154–12155. (b) Wu, Z.; Kim, H. S.; Stair, P. C.; Rugmini, S.; Jackson, S. D. On the structure of vanadium oxide supported on aluminas: UV and visible Raman spectroscopy, UV-visible diffuse reflectance spectroscopy, and temperature-programmed reduction studies. *J. Phys. Chem. B* **2005**, *109*, 2793–2800.

31 (a) Andrews, G. P.; Jones, D. S. Rheological characterization of bioadhesive binary polymeric systems designed as platforms for drug delivery implants. *Biomacromolecules* **2006**, *7*, 899–906. (b) Devon, R.; Rose Figura, J.; Douthat, D.; Kudenov, J.; Maseiko, J. Complex morphology in a simple chemical system. *Chem. Commun.* **2005**, *13*, 1678–1680.

32 Kobayashi, K.; Mustafa, G.; Tagawa, S.; Yamada, M. Transient formation of a neutral ubisemiquinone radical and subsequent intramolecular electron transfer to pyrroloquinoline quinone in the *Escherichia coli* membrane-integrated glucose dehydrogenase. *Biochemistry* **2005**, *44*, 13567–13572.

33 (a) Deamer, D. W.; Dworkin, J. P. Chemistry and physics of primitive membranes. *Top. Curr. Chem.* **2005**, *259*, 1–27. (b) Loll, B.; Kern, J.; Saenger, W.; Zouni, A.; Biesiadka, J. Towards complete cofactor arrangement in the 3.0-ÅNG. resolution structure of photosystem II. *Nature* **2005**, *438*, 1040–1044.

34 (a) Trieflinger, C.; Rurack, K.; Daub, J. Turn ON/OFF your LOV light: Borondipyrromethene-flavin dyads as biomimetic switches derived from the LOV domain. *Ang. Chem., Int. Ed.* **2005**, *44*, 2288–2291. (b) Nakajima, R.; Tsuruta, M.; Higuchi, M.; Yamamoto, K. Fine control of the release and encapsulation of Fe ions in dendrimers through ferritin-like redox switching. *J. Am. Chem. Soc.* **2004**, *126*, 1630–1631.

35 Zhang, G. Q.; Zhang, X. G.; Li, H. L. Self assembly preparation of hollow manganese dioxide and its application in zinc air battery. *J. Solid State Electrochem.* **2005**, *9*, 655–659.

36 Li, L.; King, D. L. Synthesis and characterization of silver hollandite and its application in emission control. *Chem. Mater.* **2005**, *17*, 4335–4343.

37 Cui, X.; Liu, G.; Lin, Y. Amperometric biosensors based on carbon electrodes modified with nanostructured mixed-valence manganese oxides and glucose oxidase. *Nanomedicine* **2005**, *1*, 130–135.

38 Espinal, L.; Suib, S. L.; Rusling, J. F. Electrochemical catalysis of styrene epoxidation with films of MnO<sub>2</sub> nanoparticles and H<sub>2</sub>O<sub>2</sub>. *J. Am. Chem. Soc.* **2004**, *126*, 7676–7682.



- 39 Ogasawara, T.; Debart, A.; Holzapfel, M.; Novak, P.; Bruce, P. G. Rechargeable  $\text{Li}_2\text{O}_2$  electrode for lithium batteries. *J. Am. Chem. Soc.* **2006**, *128*, 1390–1393.
- 40 Kim, H. S.; Pasten, P. A.; Gaillard, J. F.; Stair, P. C. Nanocrystalline todorokite-like manganese oxide produced by bacterial catalysis. *J. Am. Chem. Soc.* **2003**, *125*, 14284–14285.
- 41 Zitoun, D.; Pinna, N.; Frolet, N.; Belin, C. Single crystal manganese oxide multipods by oriented attachment. *J. Am. Chem. Soc.* **2005**, *127*, 15034–15035.
- 42 (a) Toberer, E. S.; Schladt, T. D.; Seshadri, R. Macroporous manganese oxides with regenerative mesopores. *J. Am. Chem. Soc.* **2006**, *128*, 1462–1463. (b) Toberer, E. S.; Seshadri, R. Spontaneous formation of macroporous monoliths of mesoporous manganese oxide crystals. *Adv. Mater.* **2005**, *17*, 2244–2246.
- 43 Omomo, Y.; Sasaki, T.; Wang, L.; Watanabe, M. Redoxable nanosheet crystallites of  $\text{MnO}_2$  derived via delamination of a layered manganese oxide. *J. Am. Chem. Soc.* **2003**, *125*, 3568–3575.